Influence of Deposition Temperature as a Reducing Agent on Synthesis of Reduced Graphene Oxide (RGO) Nanosheets

H. Darrudi and M. Adelifard
* *adelifard@du.ac.ir*

Received: February 2018 **Revised: April 2018** **Accepted: September 2018**

School of Physics, Damghan University, Damghan, Iran.

DOI: 10.22068/ijmse.16.1.22

Abstract: *In this paper we have investigated the physical properties of reduced graphene oxide (RGO) thin films prepared at various substrate temperatures of 230, 260, 290, 320 and 350 oC using spray pyrolysis technique. We have compared these films from various viewpoints, including structural, morphological, optical, electrical and thermo-electrical properties. X-ray diffraction analysis showed a phase shift from graphene oxide (GO) to RGO due to elevate the substrate temperature from 200 oC to higher temperatures, in agreement with the FTIR spectra of the layers. FESEM images of RGO thin films revealed stacked irregular folded nanosheets, and rod-like features at temperatures below and above 290 oC; respectively. Optical studies showed that the layers have a relatively high absorption coefficient (~0.8×10^4 to 1.7×10^4 cm^{-1}) in the visible range, with an optical band gap of 1.67–1.88 eV. The Hall effect data showed that all samples have a p-type conductivity with a hole concentration of ~10^{15} cm^{-3}, and sheet resistance values of about 106 Ω/square, in agreement with previous reports. The thermoelectric measurements revealed that with increasing applied temperature gradient between the two ends of the samples, the thermoelectric electromotive force (e.m.f) of the prepared RGO thin films increases.*

Keywords: *Reduced graphene oxide (RGO), Nanosheets, Optical properties, Electrical properties*

1. INTRODUCTION

Graphene, as a 2D material, has attracted increasing attention due to its unique mechanical, thermal, electrical and optical properties [1-8]. This material has a zero-band gap and 'minimum' conductivity of ~4 e^2/h even when the carrier concentration tends to be zero [9]. However, the zero-band gap of graphene limits its use in field-effect transistors in nano-electronics. Oxygen functionalization is known to tune the band gap of graphene. A gradual reduction of oxygen concentration of GO also tailors the band gap of the material as an alternative route.

There are several approaches to produce and modify reduced graphene oxide (RGO). These are: (1) fabrication of GO thin film from GO aqueous dispersion and subsequent reduction of GO films using a hot vapor of reducing agent [10-13]; (2) thermal treatment of GO to obtain "RGO"; (3) direct surface coating of GO for composites followed by a thermal or hydrothermal treatment through simultaneous reactions; and (4) chemical reduction in combination with thermal annealing to eliminate the chemical residuals and clear the patches of RGO [14]. Reducing GO at elevated temperatures (above 500 °C) was shown to reduce the oxygen concentration, but introduces defects in RGO. The main focus of this research was synthesizing high quality RGO thin films, mainly by thermal treatments via oxygen removal from GO thin films.

In our previous report, since the non-reduced GO thin films at substrate temperature below 200 °C showed insulating behavior as usual, chemical reduction was applied to make the layers conductive for different opto-electronic applications [15]. In this regards, we report a method for preparation of reduced graphene oxide (RGO) thin films by increasing substrate temperature above 200 °C (230−350 °C) without further chemical reduction in toxic atmosphere such as hydrazine vapor. We have investigated and compared the corresponding reduced samples from various viewpoints, including structural (crystallinity and surface morphology), optical (UV–Vis–near-IR absorption coefficient spectra and optical band gap estimation), electrical (carrier density and resistivity) and thermo-electrical properties.

[DOI: 10.22068/ijmse.16.1.22]

2. EXPERIMENTAL DETAILS

2. 1. Materials

Graphite (99.99%), Ethanol (99.99 %) and hydrochloric acid (37%) were supplied by Merck (Germany); Deionized water (10 MΩ cm) was also used in this way.

2. 2. Preparation of GO Suspension and Deposition of Their Thin Films

We started from GO produced by the modified Hummers method [16]. The resulting graphene oxide suspension was washed by repeated centrifugation (4000 rpm) with a hydrochloric acid (HCl, 37%) and then with deionized water and ethanol. The final suspension of graphene oxide in ethanol was rigorously sonicated for 2 min, in order to more exfoliation of the graphene oxide and prevention of the breakage of GO sheets. Then GO was dispersed in ethanol with concentration of 0.2 mg/mL and was sprayed on preheated glass substrates by spray pyrolysis instrument (Modern Technology Development Institute, Iran). The substrate temperature was varied from 230 to 260, 290, 320 and 350 °C with an accuracy of ±5 °C using a digital temperature controller. Other deposition parameters such as spray solution volume, spray deposition rate, nozzle to substrate distance and hot plate rotation speed were maintained at 100 ml, 10 ml/min, 30 cm and 50 rpm, respectively. The samples were labelled as 'RGO–230', 'RGO–260', 'RGO–290', 'RGO–320' and 'RGO–350'. An X-ray diffractometer (D8 Advance Bruker, Germany) was used to record X-ray diffraction (XRD) patterns using Cu–K alpha radiation (lambda = 0.15406 nm) in the 2theta range of 10–70deg. Spectral transmittance was recorded in the wavelength range 400–1100 nm by a Shimadzu UV1800 (Japan) spectrophotometer. The surface morphology was observed using a HITACHI S-4160 Field (Japan) Emission Scanning Electron Microscope (FESEM). The film thickness was measured using a Taly step profilometer (roughness detector with a STYLUS-Taylor Hobson model, UK). This apparatus was able to find the height of the films in a step- like configuration with a precision of about 10 nm. The electrical resistivity and Hall effect data (magnetic field strength = 200 mT) of the samples were measured in the Van der Pauw configuration [17]. Finally, by applying a temperature gradient between the two ends of the samples, the thermoelectric electromotive force (e.m.f) of the prepared films was measured, The Seebeck coefficients were determined by calculating the slope of the thermoelectric e.m.f versus temperature difference.

3. RESULTS AND DESCUSSIONS

3. 1. Structural Studies

The XRD patterns of GO and RGO thin films are presented in Fig. 1. As it shows, the pattern of GO thin film fabricated at substrate temperature of 200 °C has a high-intensity peak centered at 2θ about 10.81°. Also, the d-spacing of GO is 1.38 times larger than that of graphite, increased to 0.819 nm. The larger interlayer distance of GO than that of graphite might be due to the formation of oxygen-containing functional groups, such as hydroxyl, epoxy and carboxyl [18]. With a 30 °C increasing of substrate temperature, as seen in the XRD patterns in Fig. 1(b), it can be inferred that the typical sharp peak at 10.81° of GO thin films disappears, indicating the transformation of GO to RGO. It is worth to mention that after increasing substrate temperature, RGO230–350 samples show a broad diffraction peak at 23.32°, corresponding to the interlayer spacing of 3.82 Å. The interlayer spacing of RGO thin films were slightly larger than that of graphite, which was resulted from the small amount of residual oxygen-containing functional groups or other structural defects [19].

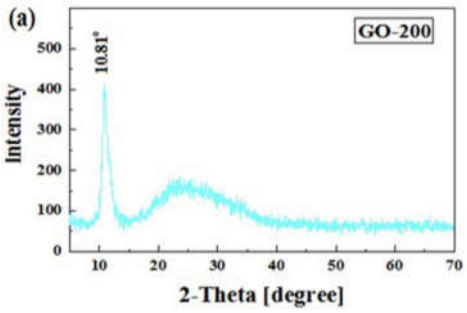

[DOI: 10.22068/ijmse.16.1.22]

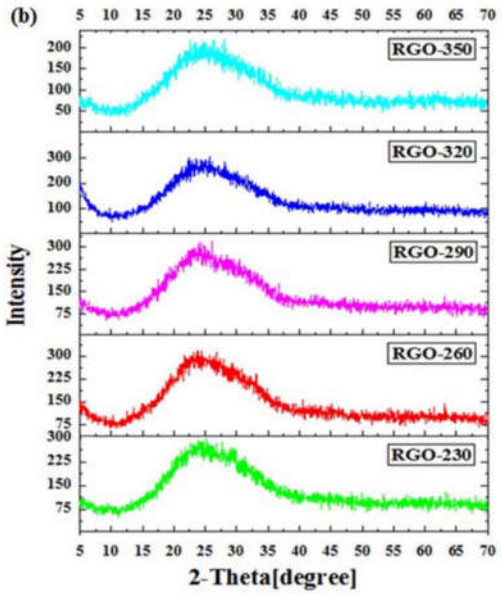

Fig. 1. XRD pattern of (a) GO and (b) RGO thin films prepared at various substrate temperatures.

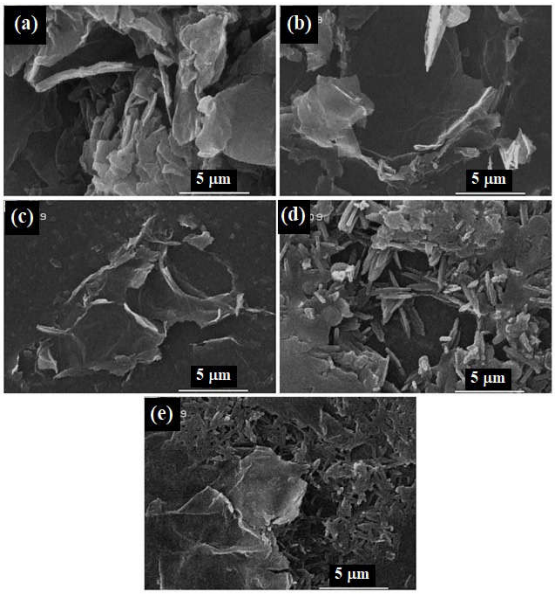

Fig. 2. FESEM images of the studied RGO thin films (a) RGO–230, (b) RGO–260, (c) RGO–290, (d) RGO–320 and (e) RGO–350.

3. 2. Morphological Studies

FESEM images of the spray-coated RGO thin film fabricated at various substrate temperatures are seen in Fig. 2 (a-e). Images reveal stacked irregular and folding nanosheets at temperatures below 290 °C. Samples RGO-320 and RGO-350 doesn't demonstrate any fluffy features, rather exhibit rod-like features in addition to the sheets.

3. 3. Optical Studies

Fig. 3 shows the spectral transmittance curves for reduced graphene oxide films. It is seen that after increasing substrate temperature the absolute transmittance of the films is increased by an amount of approximately 20-30%. This increment trend can be attributed to the difference in their morphological properties as examined by FESEM, and/or due to the increase in the density of free charge carriers which results in more absorption of light. This result is compatible with the discussions about electrical properties, section 3.4.

It is also mentioned that independent of thickness, the films show a flat optical transmittance profile at visible and near infrared region of the spectrum, making them potentially desirable for solar cell, display, and optical communication applications.

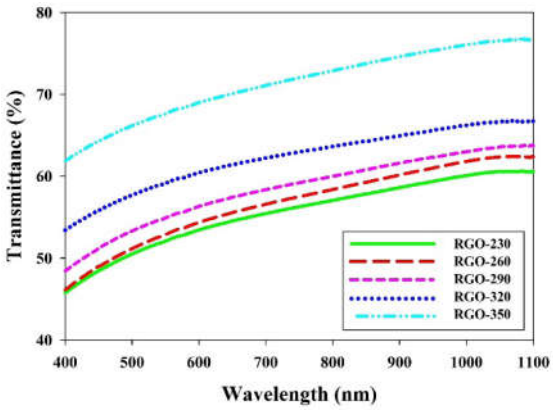

Fig. 3. Results of transmittance measurement of the RGO thin films.

Using the transmittance data, the absorption coefficient (α) could be determined by the following equation [20]:

$$\alpha = \frac{1}{d} \ln\left(\frac{1}{T}\right) \qquad (1)$$

where d, the mean thickness of the layers measured, was 400±40 nm. The variations of the absorption coefficient α, as a function of wavelength

[DOI: 10.22068/ijmse.16.1.22]

are presented in Fig. 4. As seen, the deposited layers have a relatively high absorption coefficient (~0.8×10^4 to 1.7×10^4 cm^{-1}) in the visible range.

The absorption coefficient (α) is related to the incident photon energy (hv) by the following equation [21]:

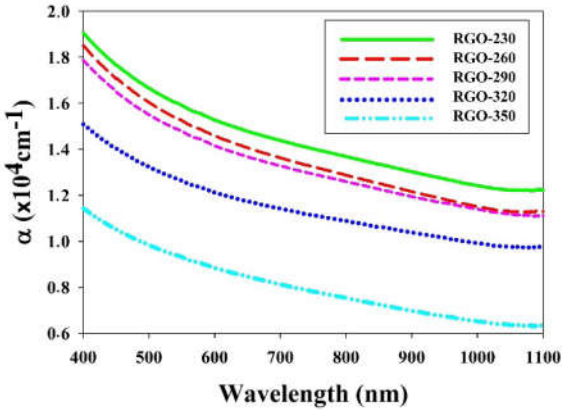

Fig. 4. The optical absorption coefficient, α (λ), for RGO thin films.

$$(\alpha hv)^2 = A(hv - E_g) \quad (2)$$

where E_g is the energy band gap and hv is the incident photon's energy.

Fig. 5 shows the variation of $(\alpha hv)^2$ versus hv of reduced graphene oxide thin films prepared at different substrate temperatures. The extracted values are presented in Table 1. The values of E_g were estimated through the intersection of the extrapolated linear part graphs with the energy axis. A glance on Table 1 and Fig. 5 shows that in contrast to the GO film (Fig. 5 (a), the RGO films prepared at substrate temperature above 200 °C exhibit lower band gap values, decrease from approximately 3.46 eV in the GO film to the range of 1.67 –1.88 eV in the RGO films. The decrease of band gap may be attributed to the change in phase (see Fig. 1); and also more oxygen vacancies, resulted from removing the oxygen-containing groups by applying higher substrate temperature, which increase the density of localized states in the band gap and consequently decrease the energy.

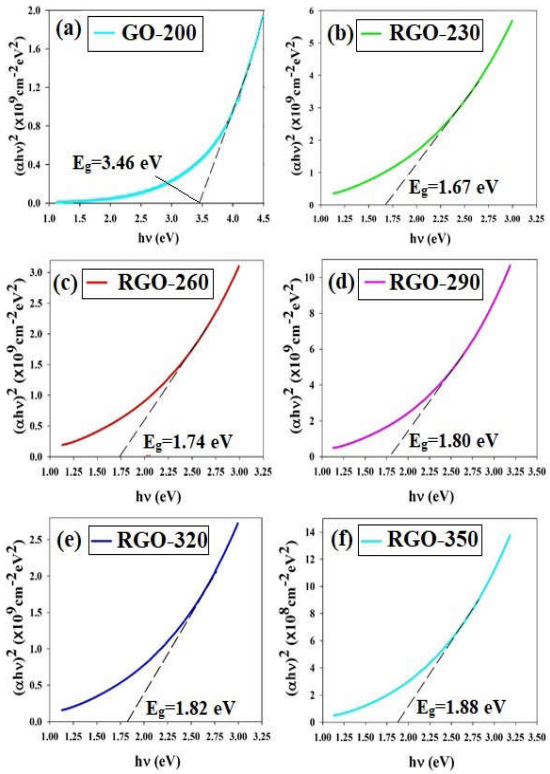

Fig. 5. The detail analysis for the optical band gap determinations in the samples (a) GO-200, (b) RGO–230, (c) RGO–260, (d) RGO–290, (e) RGO–320 and (f) RGO–350.

3. 4. Electrical Studies

The thin film prepared at substrate temperature of 200 °C (GO-200) and below showed insulating behavior as usual [15]. Since a reduction process can considerably improve the electrical conductivity of GO thin films, thermal approach, i.e. increasing the substrate temperature, was used to produce conductive RGO thin films. The effect of substrate temperature on the electrical properties of the samples was evaluated by the Hall effect and sheet resistance measurements in the Van der Pauw configuration. We found that all the studied samples exhibit p-type conductivity. The room temperature values of carrier density (p) and sheet resistance (R_s) versus the substrate temperature (and/ or sample) are given in Table 1.

[DOI: 10.22068/ijmse.16.1.22]

Table 1. optical and electrical measurement results of the RGO thin films.

Sample	Band gap energy (eV)	Sheet resistance ($\times 10^6$ Ω/square)	Carrier concentration ($\times 10^{15} cm^{-3}$)
RGO230	1.67	10.24	0.65
RGO260	1.74	6.58	1.04
RGO290	1.80	5.37	2.18
RGO320	1.82	4.13	3.99
RGO350	1.88	1.96	4.74

It is evident that while the substrate temperature of thin films increases the degenerate hole density gradually increases from ~.6.5×10^{14} cm^{-3} in RGO–230 to approximately 4.77.5×10^{15} cm^{-3} in RGO–350. Besides the estimated sheet resistances value decreases from 10.24×١٠^6 Ω/ square in RGO–230 to approximately 1.96×١٠^6 Ω/ square in RGO–350. The exact reason for this behavior is not known but this could be understood as follows. It is a well-known that various factors such as crystallinity, morphology, roughness, porosity, stress, composition, film-substrate interface, etc., play crucial roles in the electrical conductivity of the films. Hence, the variation in the electrical parameters of the films reported in the present study, with respect to substrate temperature and Ag to S molar ratio, can be attributed to the difference in their morphological properties as examined by FESEM. The R_s values of the RGO thin films are in agreement with previous reports on the electrical resistance of reduced graphene oxide thin films with chemical process [22-24].

3. 5. Thermo-Electrical studies

Fig. 6 presents the variation of the thermoelectric e.m.f versus temperature difference (δT) for RGO thin films. It can be seen that thermoelectric e.m.f. of films is increased with increasing the temperature difference between the hot and cold sides. This is obtained through increasing the carrier concentration with increasing temperature [25].

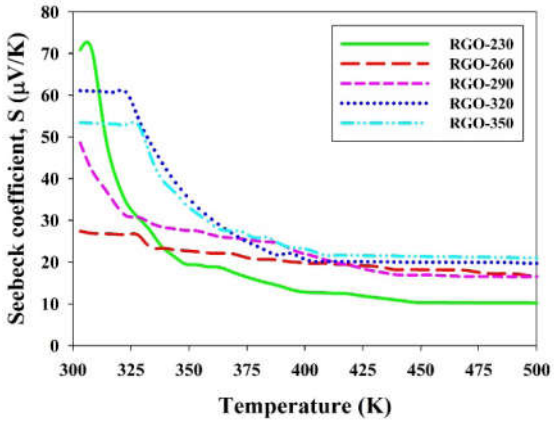

Fig. 6. Thermoelectric e.m.f versus temperature difference for the RGO thin films.

The variations of Seebeck coefficients as a function of temperature for RGO thin films are shown in Fig. 7. Variation of Seebeck coefficient at low temperatures is nearly nonlinear, which decreases slowly with a linear behavior with increasing temperature beyond 370 K. The nonlinear manner in temperatures below 370 K is related to the electron-phonon and phonon-phonon interactions, while slow linear variations are related to free electron model which are temperature dependent phenomena [26].

3. 6. FTIR Studies

The FTIR spectra obtained for the graphene oxide (GO) and reduced graphene oxide (RGO) are shown in Fig. 8. The existence of oxygen groups in graphene oxide FTIR spectrum was affirmed by

[DOI: 10.22068/ijmse.16.1.22]

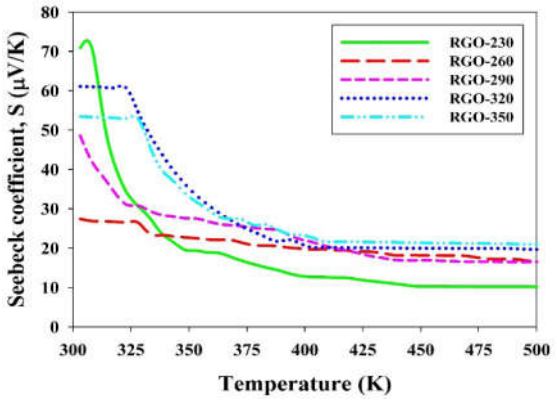

Fig. 7. Seebeck coefficient versus temperature for the RGO thin films.

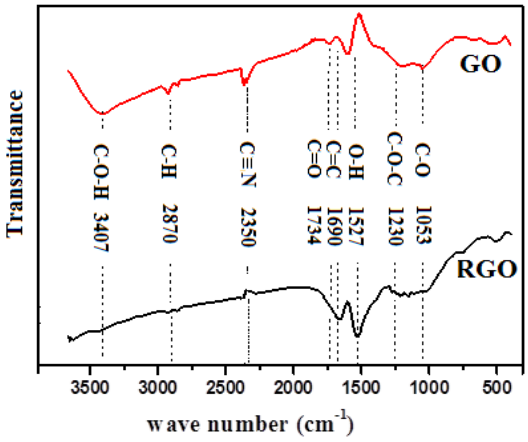

Fig. 8. FTIR spectra for GO and RGO.

the peaks observed at 1053, 1230, 1734 and 3407 cm^{-1} corresponds to C–O (vibrational mode), C–O–C (breathing vibrations from epoxy groups), C=O (stretching vibration band from carbonyl and carboxyl groups), and C–O–H (stretching vibration), respectively. Also, a narrow peak with the maximum at 2870 cm^{-1} in the upper spectrum was identified to be due to the C−H bonding from hydroxyls and trapped water molecules in the GO sample. For the reduced graphene oxide, this peaks are disappeared due to the partial removal of hydroxyl groups as well as water molecules by chemical reduction. On the other hands, the increased peak intensity of C=C stretching upon reduction suggests the recovery of sp2 lattice,_while the markedly weaker bands of adsorbed water and oxygen groups confirm their removal. Nevertheless, the O–H bending mode from hydroxyl groups was still observed in reduced material. The removal of oxygen functionalities after reduction is confirmed by the corresponding weaker bands in reduced materials.

4. CONCLUSION

Reduced graphene oxide thin films were prepared by spray–coated GO dispersion at various substrate temperatures from 230 to 350 °C. X–ray analysis showed that with increasing substrate temperature from 200 °C to higher substrate temperatures typical sharp peak for GO thin film at approximately 10.81° disappears, indicating the transformation of GO to RGO. FESEM images of the spray-coated RGO thin film revealed stacked irregular and folding nanosheets at temperatures below 290 °C; however, it changed to rod-like features in addition to the sheets at temperatures above 290 °C. Optical measurements showed absorption coefficient values as high as ~10^4 cm^{-1}. Also, the direct optical band gap in average increases from 1.67 eV to 1.88 eV. Finally, the Hall experiment data showed that all the reduced thin films have a *p*-type conductivity with a carrier density of about 10^{15} cm^{-3}, and sheet resistance values of about 10^6 Ω/square, in agreement with previous reports on the electrical resistance of chemically reduced graphene oxide thin films. The thermoelectric measurements showed that while variation of Seebeck coefficient at low temperatures is nearly nonlinear, it changes to linear manner at temperatures above 370 K.

REFERENCES

1. Lightcap, I. V., Kosel, T. H. and Kamat, P. V., "Anchoring Semiconductor and Metal Nanoparticles on a Two-Dimensional Catalyst Mat. Storing and Shuttling Electrons with Reduced Graphene Oxide". Nano Lett., 2010, 10, 577-583.
2. Ng, Y. H., Lightcap, I. V., Goodwin, K., Matsumura, M. and Kamat, P. V., "To What Extent Do Graphene Scaffolds Improve the Photovoltaic and Photocatalytic Response of TiO_2 Nanostructured Films?", J. Phys. Chem. Lett., 2010, 1, 2222-2227.
3. Hu, Y. H., Wang, H. and Hu, B., "Thinnest Two-Dimensional Nanomaterial—Graphene for Solar Energy", Chem. Sus. Chem. 2010, 3, 782-796.
4. Su, C., Xu, Y., Zhang, W., Zhao, J., Tang, X., Tsai, C. and Li, L., "Electrical and Spectroscopic Characterizations of Ultra-Large Reduced Graphene

[DOI: 10.22068/ijmse.16.1.22]

Oxide Monolayers". Chem. Mater., 2009, 21 (11), 5674-5680.
5. Zhu, Y., Cai, W., Piner, R. D., Velamakanni, A. and Ruoff, R. S., "Transparent self-assembled films of reduced graphene oxide platelets", Appl. Phys. Lett., 2009, 95 (10), 103104-103107.
6. Li, X. L., Wang, X. R., Zhang, L., Lee, S. W. and Dai, H. J., "Chemically derived, ultrasmooth graphene nanoribbon semiconductors", Science, 2008, 319, 1229-1232.
7. Park, M. D., Zhu, S. J., An, Y. W., J. H. and Ruoff, R. S., "Graphene-Based Ultra capacitors", Nano Lett., 2008, 8, 3498-3502.
8. Freitag, M., "Graphene: nanoelectronics goes flat out", Nat. Nanotechnol., 2008, 3, 455-457.
9. Geim, A. K and Novoselov, K. S. "The rise of graphene". Nat. Mater., 2007, 6, 183-185.
10. Eda, G., Fanchini, G. and Chhowalla, M., "Large-area ultrathin films of reduced graphene oxide as a transparent and flexible electronic material", Nat. Nanotechnol., 2008, 3, 270-274.
11. Becerril, H. A., Mao, J., Liu, Z., Stoltenberg, R. M., Bao, Z. and Chen, Y., "Evaluation of solution-processed reduced graphene oxide films as transparent conductors", ACS Nano, 2008, 2, 463-470.
12. Cote, L. J., Kim, F. and Huang, J., "Langmuir–Blodgett Assembly of Graphite Oxide Single Layers", J. Am. Chem. Soc., 2009, 131, 1043-1049.
13. Watcharotone, S., Dikin, D. A., Stankovich, S., Piner, R., Jung, I., Dommett, G. H. B., Evmenenko, G., Wu, S. E., Chen, S. F. and Liu, C. P., "Graphene-silica composite thin films as transparent conductors", Nano Lett., 2007, 7, 1888-1892.
14. Acik, M. and Chabal1, Y. J., "A Review on Reducing Graphene Oxide for Band Gap Engineering", J. Mater. Sci. Res., 2013, 2 (1), 101-111.
15. Adelifard, M. and Darudi, H., "A facile fabrication of chemically converted graphene oxide thin films and their uses as absorber materials for solar cells", Appl. Phys. A, 2016, 122, 682.
16. Hummers, W. S., Offeman, R. E., Am. Chem, Soc, J., 1958. 80, 1339.
17. Van der Pauw, L. J., "A method of measuring specific resistivity and Hall effect of discs of arbitrary shape", Philips. Res. Repts. 1958, 13, 1-9.
18. Tong, X., Wang, H., Wang, G., Wan, L., Ren, Z. and Bai, J., "Controllable synthesis of graphene sheets with different numbers of layers and effect of the number of graphene layers on the specific capacity of anode material in lithium-ion batteries", J. Solid State Chem., 2011, 184, 982-989.
19. Gao, W., Alemany, L. B., Ci, L. and Ajayan, P. M., "New insights into the structure and reduction of graphite oxide", Nat. Chem., 2009, 1, 403-408.
20. Manoj, P. K., Joseph, B, Vaidyan, V. K. and Sumangala Devi Amma, D., " Preparation and characterization of indium-doped tin oxide thin films", Ceram. Int., 2007, 33, 273-278.
21. Tauc, J., "Amorphous and Liquid Semiconductors", Plenum Press, New York, 1974, 159-220.
22. Gilje, S., Han, S., Wang, M., Wang, K. L.and Kaner, R. B. "A Chemical Route to Graphene for Device Applications", Nano Lett. 2007, 7, 3394-3398.
23. Li, D., Muller, M. B., Gilje, S., Kaner, R. B. and Wallace, G. G.,"Processable aqueous dispersions of graphene nanosheets", Nat. Nanotechnol., 2008, 3, 101-105.
24. Shi, H. F., Wang, C., Sun, Z., Zhou, Y., Jin, K. and Yang, G., "Transparent conductive reduced graphene oxide thin films produced by spray coating", Sci. China-Phys. Mech. Astron., 2015, 58, 14202-14206.
25. Patil, P. S. and Kadam, L. D., "Preparation and characterization of spray pyrolyzed nickel oxide (NiO) thin films", Appl. Surf. Sci., 2002, 199, 211-221.
26. Bagheri-Mohagheghi, M. M, Shahtahmasebi, N., Alinejad, M. R., Youssefi, A. and Shokooh-Saremi, M., "Fe-doped SnO2 transparent semi-conducting thin films deposited by spray pyrolysis technique: Thermoelectric and p-type conductivity properties", Solid. State. Sci., 2009, 11, 233-239.

[DOI: 10.22068/ijmse.16.1.22]